Environmental Modelling and Software 139 (2021) 104994

Contents lists available at ScienceDirect

Environmental Modelling and Software

journal homepage: http://www.elsevier.com/locate/envsoft

A rapid 3D reproduction system of dam-break floods constrained by post-disaster information

Weilian Li [a], Jun Zhu [b,*], Lin Fu [a], Qing Zhu [a], Yukun Guo [a], Yuhang Gong [b]

[a] Faculty of Geosciences and Environmental Engineering, Southwest Jiaotong University, West Park of Hi-Tech Zone, 611756, Chengdu, China
[b] Sichuan Institute of Land Science and Technology (Sichuan Center of Satellite Application Technology), Department of Natural Resources of Sichuan Province, 189 Wanfeng Road, 610045, Chengdu, China

ARTICLE INFO

Keywords:
Post-disaster information
Dam-break flood
Spatiotemporal process
Rapid reproduction
3D visualization

ABSTRACT

The 3D reproduction of dam-break floods plays a key role in emergency management and disaster information dissemination. However, existing systems for the simulation of floods have some deficiencies. First, the input data parameters are complex. Second, the simulation process is cumbersome and time consuming, and it lacks a complete workflow. In this paper, we develop a platform for the rapid 3D reproduction of dam-break floods. Key technologies, such as numerical models of dam-break floods based on cellular automata (CA), 3D reproduction constrained by post-disaster information, and dynamic augmented representation, are discussed in detail. Then, two typical dam-break flood cases are selected for experimental analysis. The experimental results show that the system can support the rapid 3D reproduction of dam-break floods constrained by post-disaster information. Compared with that of other simulation systems, the reproduction time is reduced to less than 1 h, and this system supports rapid reproduction at different times and positions.

1. Introduction

The frequency and intensity of global extreme events have increased dramatically due to climate change and rapid economic growth. Floods are the most common and widespread type of natural disasters (Patel and Srivastava, 2013; Wan et al., 2014; Qiu et al., 2017). Dam-break floods are flood disasters that are usually associated with barrier lakes and obsolete reservoirs and are characterized by sudden occurrence, rapid expansion, high velocity and severe destruction (Li et al., 2013). As dam-break floods are a complex geographical phenomenon, the spatiotemporal process is often more important than the final spatial pattern, only the development process is clearly understood, and the deep-level change rules merit further exploration (Li et al., 2009).

Simulations have become a fundamental method for gaining insight into complex geographic processes (Bainbridge 2007; Chen et al., 2020). Moreover, developments in information science, earth observation technologies and geographical information science have strengthened the connections among geographical data, models and visualization, providing new perspectives and opportunities for spatiotemporal process modeling and the visualization of dam-break floods (Goodchild 2004; Li 2012; Chen et al., 2015; Achu et al., 2020; Kaur et al., 2019; Lü et al., 2019).

Many types of research have been conducted on flood simulation, with studies employing 1D hydraulic models, 2D hydraulic models, 1D-2D coupled hydraulic models and hydrological models. Most work has focused on simulation prediction and early warning of flood processes under ideal conditions (Ernst et al., 2010; Domingo et al., 2010; Pasquier et al., 2018; Wang et al., 2018). In practical use, it is difficult to use predictive models due to the uncertainty of data parameters, the instability of model structure, and the complexity of external conditions. Consequently, there is no universal method or software that can be applied to accurately predict floods under different conditions.

Disaster reproduction is a restored representation of the reason the disaster occurred, the process and the results. Whereas disaster simulation is forward-looking and focuses on the prediction of disaster evolution process, disaster reproduction emphasizes the restored representation of the disaster spatiotemporal process based on post-disaster information. The latter is mainly used for post-disaster education and media promotion, an intuitive and detailed 3D reproduction of the disaster process can improve the transmission efficiency of disaster information. Thus, disaster reproduction can overcome the shortcomings of traditional disaster education materials, which overly rely on 'image and text publicity', and ultimately improve people's disaster risk awareness and disaster prevention capabilities. After a dam-break flood,

* Corresponding author.
E-mail address: zhujun@swjtu.edu.cn (J. Zhu).

https://doi.org/10.1016/j.envsoft.2021.104994
Accepted 13 February 2021
Available online 25 February 2021

post-disaster information, such as the dam-break location, storage capacity, and affected area and buildings, can be used to help improve the simulation model of disasters (Li et al., 2015), thereby improving the spatiotemporal reproduction accuracy for this flood type. Moreover, transferring the disaster risk knowledge implied in numerical results to decision makers and the general public is a difficult task. The 3D virtual environment can intuitively display the simulation results of floods, which can improve users' perception and cognitive understanding of a dam-break flood disaster (Cheng et al., 2019; Chen et al. 2013, 2015, 2018; Havenith et al., 2019; Bailey and Chen, 2011; Lin et al., 2013a). Existing flood simulation software (e.g., FLO2D, HEC-RAS, etc.) emphasizes risk prediction, and problems with its application include tedious data processing, long simulation times and a high degree of specialization. Therefore, a rapid dam-break flood reproduction system that integrates data processing, simulation calculation and dynamic representation is urgently needed to support emergency decisions and the dissemination of risk knowledge.

This paper outlines the design and implementation of a rapid dam-break reproduction system. The system integrates a dam-break numerical model based on the cellular automata (CA) and the virtual geographic environment (VGE) framework, realizes rapid reproduction and augmented representation of a dam-break flood under the constraints of post-disaster information, and provides decision-making information support and risk knowledge for disaster-related persons. To realize the high-efficiency reproduction of a whole dam-break flood process, this system integrates data acquisition, model calculation and dynamic visualization functions. Through a user-friendly operation interface and flexible parameter configuration, the whole process of a dam-break flood can be represented in virtual 3D view. A dam-break flood that occurs anytime and anywhere can be rapidly reproduced by this system, and the reproduction time is reduced to less than 1 h, which greatly improves the 3D restoration efficiency of the spatiotemporal evolution of disasters.

2. Related works

Information systems play a significant role in flood disaster management (Granell et al., 2013; Ding et al., 2015). Disaster management mainly includes four stages, prevention, preparedness, response and recovery, with different flood information systems serving different stages (Carter 2008; Pearce 2003). Serving the prevention and preparation stages of flood disaster management are flood prevention and early warning systems formed by integrating atmospheric models, hydraulic models, hydrological models and sensor monitoring data (Qiu et al., 2017; Kauffeldt et al., 2016; Huang et al., 2015). These types of systems are usually guided by the government and completed by integrating multidisciplinary and multisection collaboration. The common characteristics of the Chinese National Disaster Reduction System, the British National Flood Forecasting System and the European Flood Warning System (Fan et al., 2016; Ding et al., 2015; Price et al., 2012; Bartholmes et al., 2009) are powerful system functions, complex architecture and high usage permission, limiting their accessibility to general engineering users and researchers. Other systems focus on the simulation, prediction and risk assessment of floods and have been widely used by researchers and local organizations for flood risk management. For example, Environmental Fluid Dynamics Code (EFDC) is an open source software for 1D/2D/3D hydrodynamics and water quality simulation, it has the advantages of simple system integration and high computational efficiency but exhibits poor performance in fitting complex terrain and irregular boundaries (Shin et al., 2019; Yin and Seo, 2016). The MIKE series is currently the most mature and widely used commercial software in the water conservancy industry, and it mainly includes three modules: MIKE-11, MIKE-21 and MIKE-FLOOD. Among them, MIKE-21 is used mainly for 2D flood simulation with high precision, but it has low computational efficiency and cannot be readily integrated with other flood management systems (Warren and Bach, 1992; Symonds et al., 2016). The Hydrologic Engineering Center (HEC) is a series of hydraulic engineering application software packages with different application fields from HEC-1 to HEC-6, and it includes the HEC-geoRAS extension module that was developed in association with the ESRI company. HEC-geoRAS has established a bridge for data exchange between the HEC-RAS system and ArcGIS platform, and it is mainly used for preprocessing input data and postprocessing simulation results, which improves the efficiency of simulation and visualization. However, the input parameters of HEC-geoRAS are complex, requiring not only geographic data but also hydrological and hydraulic data, and three independent systems are used in this module to work with input data, process simulation and visualization separately (Sharma and Majumdar, 2016; Thakur et al., 2017).

GeoDam-BREACH is a GIS toolkit for dam-break modeling, emergency action formulation and consequence assessment. It supports inputting 2D simulation data of HEC-RAS and integration of ArcGIS, but it does not provide support for users not associated with the Federal Emergency Management Agency (FEMA (2013)). FLO-2D is a 2D simulation software package for flood and debris flow disasters that has been widely used in fluid simulation (Wu et al., 2013). Delft 3D, a software package for the water environment developed by Delft University in the Netherlands, is considered the most advanced 3D hydrodynamic-water quality model system in the world. It mainly includes Delft 3D-FLOW, Delft 3D-WAVE, Delft 3D-WAQ and other modules, which have high degrees of integration and interoperability as well as good stability and fast speed (Symonds et al., 2016; Waldman et al., 2017), but the simulation process is complex and requires many parameters. During disaster response, it is difficult to obtain substantial data in a short time, which makes Delft 3D difficult to apply to a dam-break flood. In summary, the main shortcomings of the current flood disaster systems for rapid reproduction are as follows: 1) the input data parameters are various and complex, 2) the simulation process is cumbersome and time consuming, and 3) the data-simulation-visualization process lacks a complete workflow.

3. Methodology

3.1. Overall research framework

Fig. 1 shows the overall research framework of this paper, which includes three main parts. First, the required parameters for simulation of the whole dam-break flood process are obtained based on remote sensing images and digital elevation model (DEM) data, which include the landslide body, disaster boundary, affected buildings, etc. These data are the basis for the reproduction and representation of the dam-break flood. Second, the cellular automata model of a dam-break flood is constructed, and the reproduction of the dam-break spatiotemporal process is constrained by post-disaster information (e.g., the storage capacity and disaster range). Finally, based on the virtual geographical environment, the whole dam-break flood process is dynamically visualized through the combination of static and dynamic representations, which maximizes the efficiency of flood disaster information transmission and perception.

3.2. The 3D reproduction of the dam-break flood process constrained by post-disaster information

3.2.1. Numerical model of dam-break floods based on CA

Compared with the common hydraulic model and hydrological model, the numerical model of the dam-break flood based on CA has the advantages of high parallelism, convenient boundary handling and simpler arithmetic (Li et al. 2013, 2015). In this paper, a 2D cellular automata is used to simulate the evolution of a dam-break flood in a discrete time-space framework (Li et al. 2012, 2013, 2015; Zhu et al., 2015). Fig. 2 shows the structure of the CA-based numerical model of a dam-break flood, which includes four main parts: cell space,

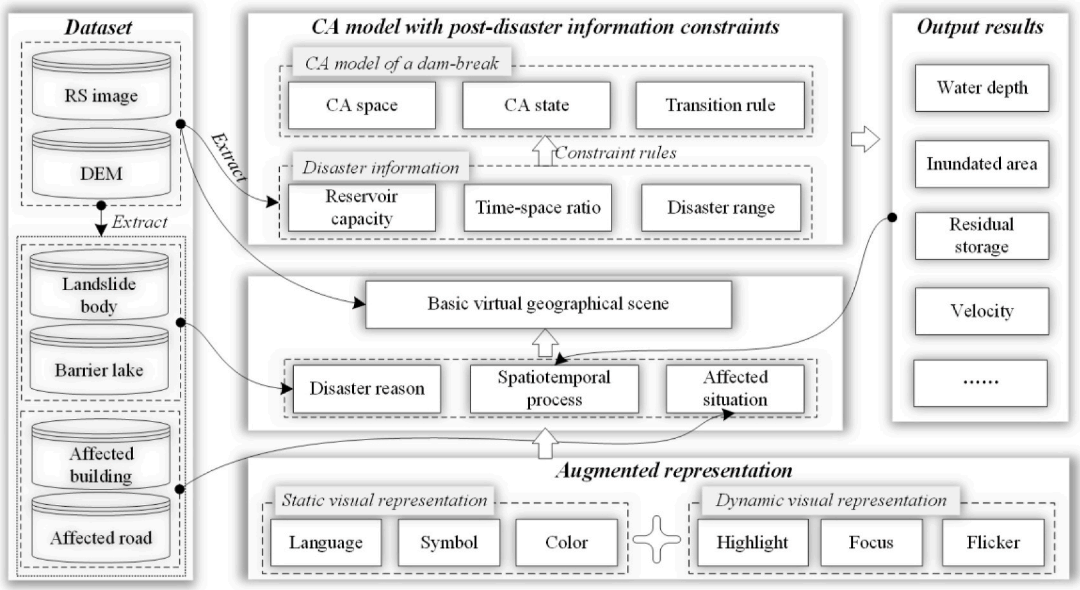

Fig. 1. Overall research framework.

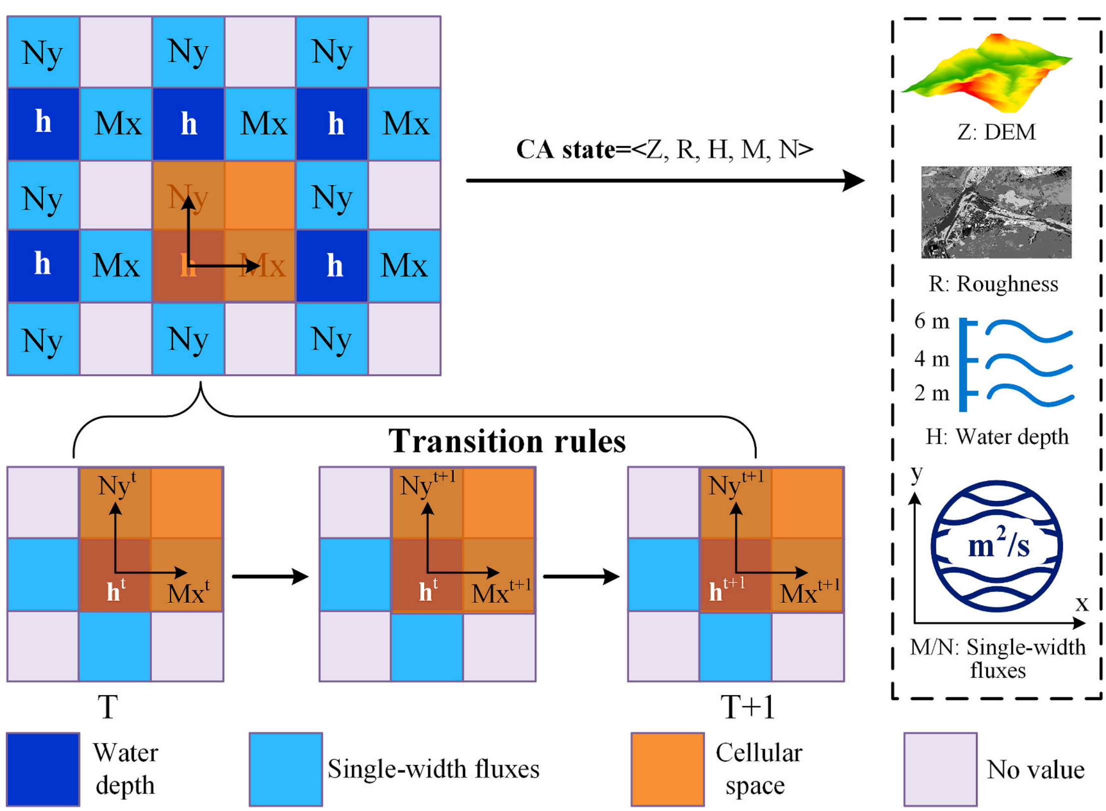

Fig. 2. The model structure of a dam-break flood.

neighborhood, cell state and transition rules.

(1) Cell space and neighborhood

The research area is uniformly divided into grid elements within a square, each element represents a cell, and four adjacent cells form a cell space, which includes water depth and single-width flow in the X and Y directions. In addition, the Von Neumann type is used to update the cell state.

(2) Cell state

The cell state of a dam-break flood can be represented by a five-tuple, as shown in formula (1).

$$C_{state} = \langle Z, R, H, M, N \rangle \tag{1}$$

In this formula, C_{state} represents the cell state, Z represents the elevation value of the cell, R indicates the roughness value, H indicates the water depth, M indicates the single-width fluxes in the X direction, and N represents the single-width fluxes in the Y direction.

(3) Transition rules

The transition rules between cells are solved by the Saint-Venant equations. The calculation process includes the following three steps:

① Set the initial parameters of the break cell. All cells are considered waterless areas except for the break cell, the water depth and single-width fluxes are set to zero.
② Use the water depth of the CA cell, single-width fluxes, flow velocity and water surface elevation at time t to calculate the cell single-width fluxes ($M_{i,j}^{t+1}$ and $N_{i,j}^{t+1}$) at time t+1. The calculation method is shown in formula (2).

$$\begin{cases} M_{i,j}^{t+1} = M_{i,j}^{t} - g\dfrac{\Delta t\left(h_{i+1,j}^{t} + h_{i,j}^{t}\right)\left(z_{i+1,j}^{t} - z_{i,j}^{t}\right)}{\Delta x} - gn_{i,j}^{2}\dfrac{\overline{u_{i,j}}\Delta t\sqrt{\left(u_{i,j}^{t}\right)^{2} + \left(v_{i,j}^{t}\right)^{2}}}{\left[\left(h_{i+1,j}^{t} + h_{i,j}^{t}\right)/2\right]^{\frac{1}{3}}} \\ N_{i,j}^{t+1} = N_{i,j}^{t} - g\dfrac{\Delta t\left(h_{i,j+1}^{t} + h_{i,j}^{t}\right)\left(z_{i,j+1}^{t} - z_{i,j}^{t}\right)}{\Delta y} - gn_{i,j}^{2}\dfrac{\overline{v_{i,j}}\Delta t\sqrt{\left(u_{i,j}^{t}\right)^{2} + \left(v_{i,j}^{t}\right)^{2}}}{\left[\left(h_{i,j+1}^{t} + h_{i,j}^{t}\right)/2\right]^{\frac{1}{3}}} \end{cases} \tag{2}$$

In the formula, $M_{i,j}^{t+1}$ and $N_{i,j}^{t+1}$ represent the single-width fluxes (m^2/s) of the cell (i, j) in the X direction and the Y direction, respectively, at time t; $h_{i,j}^{t}$ represents the water depth (m) of the cell (i, j) at time t; $z_{i,j}^{t}$ represents the water surface elevation (m); $u_{i,j}^{t} = M_{i,j}^{t}/h_{i,j}^{t}$ and $v_{i,j}^{t} = N_{i,j}^{t}/h_{i,j}^{t}$ represent the velocity of the cell (i,j) in the X direction and Y direction (m/s), respectively; Δt and the Δx, Δy pair indicate the iteration unit time and cell size(m), respectively; g indicates the gravitational acceleration; and $n_{i,j}^{2}$ indicates the roughness of the cell (i,j) (m$^{-1/3}$s).

$$h_{i,j}^{t+1} = h_{i,j}^{t} - \frac{\Delta t\left(M_{i+1,j}^{t+1} - M_{i,j}^{t+1}\right)}{\Delta x} - \frac{\Delta t\left(N_{i,j+1}^{t+1} - N_{i,j}^{t+1}\right)}{\Delta y} \tag{3}$$

③ Once the single-width fluxes $M_{i,j}^{t+1}$ and $N_{i,j}^{t+1}$ at time t+1 are obtained, the water depth of the cell (i, j) at time t+1 can be calculated using formula (3). Through iterative calculation of the above formula, the water depth value of the cell over continuous time can be obtained.

3.2.2. Reproduction of dam-break floods constrained by post-disaster information

Abundant disaster information (e.g., the range and arrival time) can be obtained from post-disaster geographic data. This information can be used to constrain the spatiotemporal evolution of a flood, thereby enhancing the visual effect of dam-break flood reproduction. This paper takes the water storage, disaster boundary and time-space ratio as constraint rules.

(1) Water storage balance

During the evolution of a dam-break flood, the total flood amount remains constant, that is, the total amount of flood is equal to the sum of cell water and the residual water, as shown in formula (4).

$$V_{total} = V_{residual} + V_{cell} * Num \tag{4}$$

In the formula, V_{total} represents the total flood volume, $V_{residual}$ represents the remaining amount, V_{cell} represents the cell volume with water, and *Num* represents the number of cells with water. If the sum of the remaining and the cell volume is not equal to the total flood amount, we dynamically allocate the surplus or reduced water to the cells based on the preset storage capacity to maintain the total balance.

(2) Disaster boundary

Fig. 3 illustrates the main concept of the disaster boundary constraint, the blue lines represent disaster boundaries. This constraint provides two benefits: it reduces unnecessary calculations, thereby improving the calculation efficiency of the model, and it improves the reproduction effect and accuracy. In this paper, the elevation value of the boundary cell is set to 9999 and is regarded as an invalid cell, as shown in Fig. 3 and formula (5).

$$\mathrm{G_{value}} = \begin{cases} Nodata & G_{i,j} = 9999 \\ Depth & G_{i,j}! = 9999 \end{cases} \tag{5}$$

In the formula, $\mathrm{G_{value}}$ represents the water depth of the cell, and $G_{i,j}$ represents the elevation of the cell. If the elevation of the cell is 9999, it is not involved in the iterative calculation.

(3) Time-space ratio

The time-space ratio is used to describe the relationship between the iteration time of the cell and the real evolution time. When the dam-break flood starts to flow, the water velocity often increases, and a larger time-space ratio is used to obtain a smaller time step. As the dam-break flood progresses, the water velocity gradually decreases, and a large time interval is required to adopt the flow rate. Therefore, it is necessary to dynamically change the value of the space-time ratio during iterative calculation, as shown in formula (6).

$$\Delta t = \frac{\Delta s}{st_{ratio}\{st1, st2, \ldots\}} \tag{6}$$

In the formula, Δt represents the unit time step of the cell iterative calculation, Δs represents the cell scale, and st_{ratio} represents the time-space ratio. st1 and st2 indicate two values of the time-space ratio. In this paper, the initial value was set to 100.

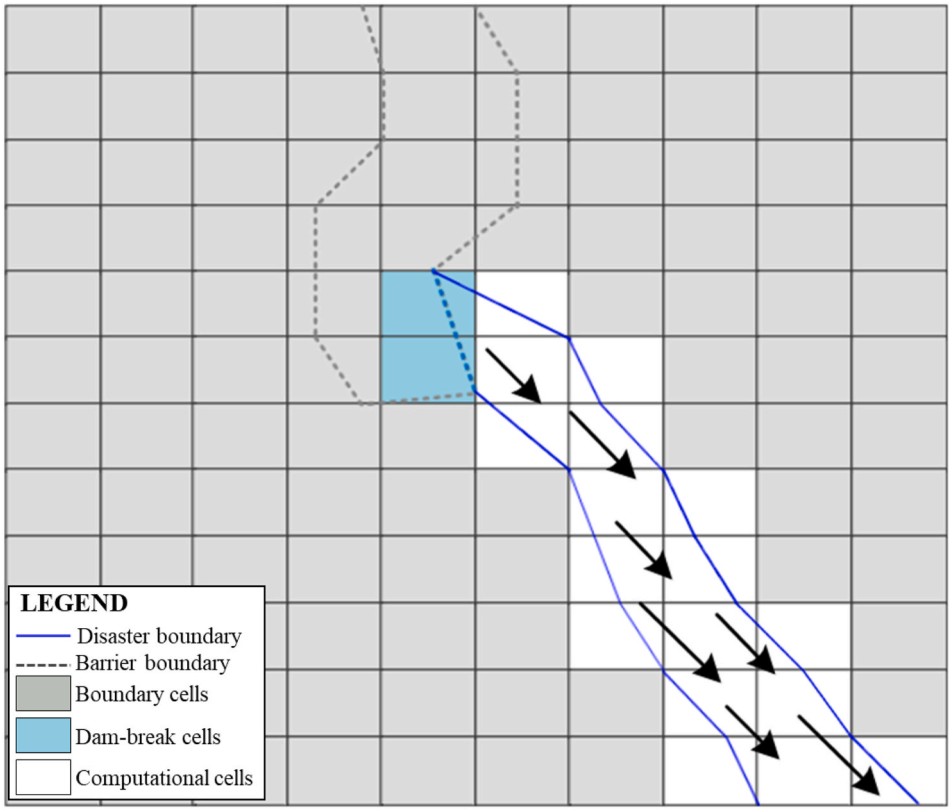

Fig. 3. Disaster boundary constraint.

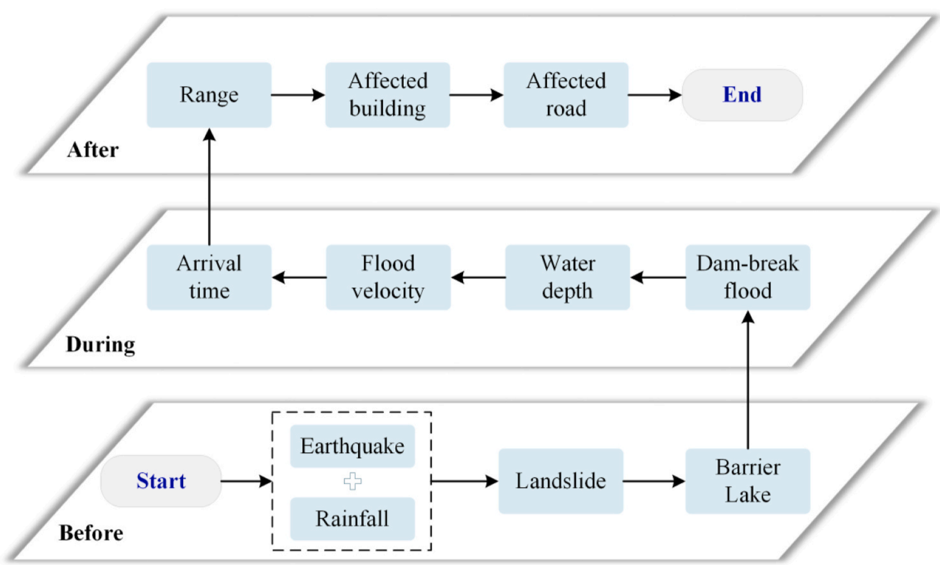

Fig. 4. Logical description of the whole process of a dam-break flood.

3.3. Augmented representation of the whole process of a dam-break flood integrated with the VGE framework

3.3.1. Logical description of the whole process of a dam-break flood

Story maps can relay information about times, places, questions and tendencies in a clear, intuitive and interactive manner under the background of a geographical environment. This paper draws lessons from the core idea of story maps and divides the whole flood disaster process into three parts: the disaster cause, spatiotemporal process and disaster situation. By describing relationships by using correct causal logic and context, the whole process of the disaster is described in the narrative manner of storytelling. A logical description of a whole process of a dam-break flood is shown in Fig. 4. Earthquakes and intense rainfall induce landslides and the formation of a barrier lake. As the water level continues to rise, dam-breaking floods erupt. With the evolution of the flood, disaster information such as water depth, flow rate and arrival time are represented, and finally, the affected buildings and affected roads are represented.

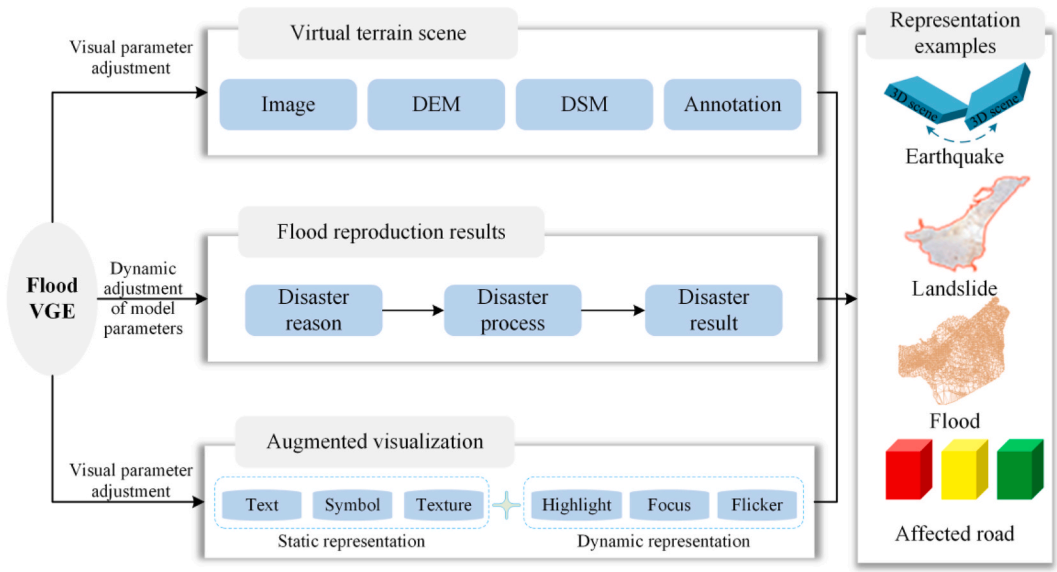

Fig. 5. Augmented representation of dam-break floods.

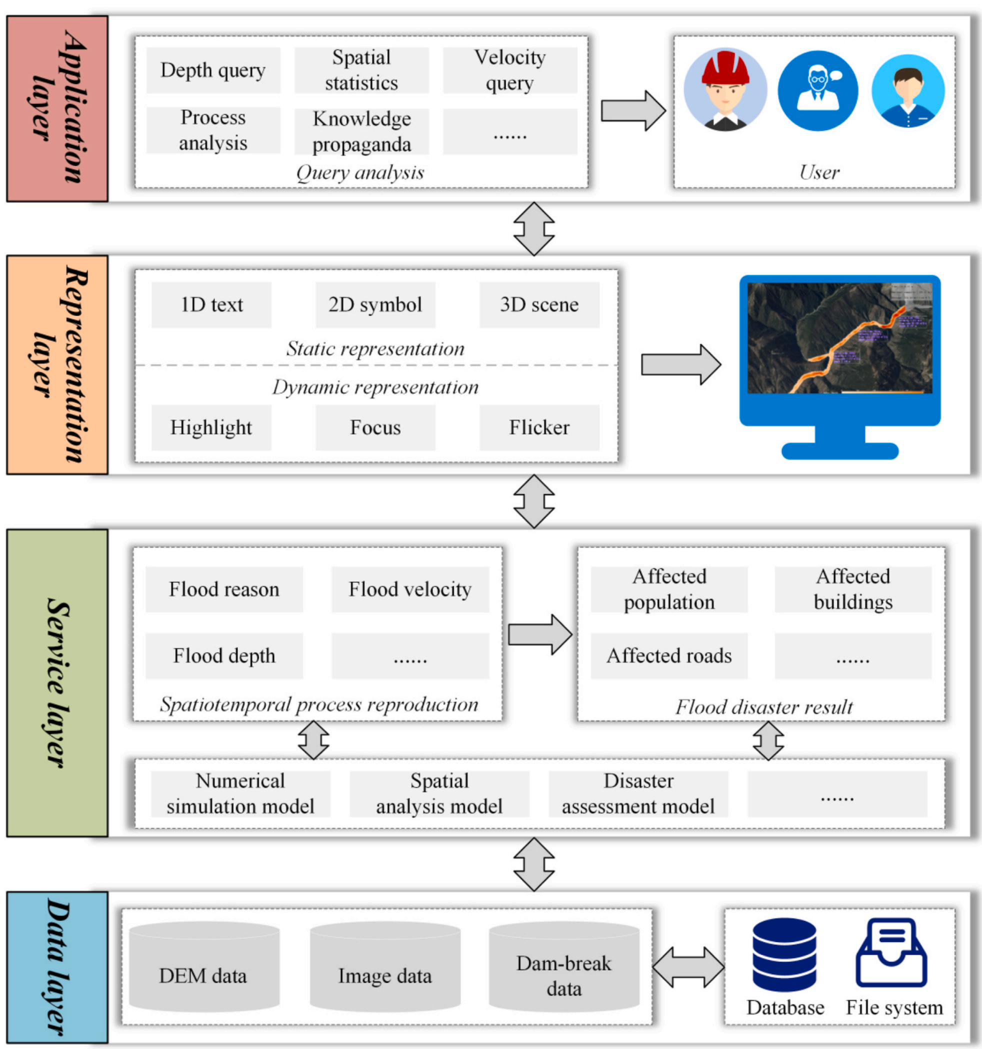

Fig. 6. The system architecture.

3.3.2. *Augmented representation of dam-break floods integrated with the VGE framework*

As a new generation of GIS theoretical frameworks, VGE focuses on spatial data sharing, geographic model integration and multiscale, all-round interactive visualization (Lin et al. 2013b, 2015; Lü et al., 2019). Based on the VGE framework, the calculation and visualization of a dam-break flood can be tightly integrated, and the framework supports disaster data processing, flexible configuration of simulation parameters and visual analysis of calculation results.

Augmented representation is used to improve the interpretation ability of scene data through text, symbols, etc., so that users can see the essence of scene data (Li et al., 2019a). The augmented representation of the dam-break flood takes the virtual terrain scene as the carrier, and the simulation results of the flood are merged into the 3D virtual scene according to the causal logic and time axis, as shown in Fig. 5. In addition to presenting conventional static information, the scene presents a combination of static representation (e.g., text, symbols, and texture) and dynamic representation (e.g., highlight and focus), which can dynamically reveal the spatiotemporal laws of disasters and enable semantic enhancement and deep focus on flood disaster information, thus helping users quickly master key information and improve their disaster awareness (Li et al. 2019b, 2020).

4. System implementation and application cases

4.1. *System architecture*

The architecture of the dam-break flood reproduction system is divided into four main layers, as shown in Fig. 6. The data layer is the foundation of the system, which adopts the mixed storage of a file system and PostgreSQL database. The service layer is the core of the system and is responsible for the processing and integration of relevant models. The representation layer provides multidimensional spatiotemporal visualization and augmented representation of the dam-break flood process to improve the transmission efficiency and spatial cognition of disaster information. The application layer is oriented towards users involved in dam-break flood management. Through simple parameter configurations and user-friendly interactive interfaces, users can query and analyze flood disaster information.

4.2. *System implementation*

The dam-break flood reproduction system was developed using the C++ language on the Visual Studio 2010 platform, and the operation interface was written in QT 5.8. The data processing tool was developed based on ArcEngine 10.2, and the OSG toolkit was used to build a 3D scene visualization platform for the dam-break flood disaster. The system interface is shown in Fig. 7.

The system was divided into three parts: a functional module, a layer management module and a display area. The functional module supports mainly data processing, parameter configuration and model calculation. The layer management module on the left supports layer visibility and rendering order settings. The display area provides augmented visualization of the entire process of the dam-break flood.

4.3. *Application experiments*

4.3.1. *Study area*

As shown in Fig. 8, two study areas were selected for experimental analysis. Detailed descriptions are presented below.

(1) Case 1

On October 10th, 2018, a large-scale landslide occurred in the Jinsha River Basin at the border of Sichuan and Tibet. The landslide blocked the main stream of the Jinsha River and caused the formation of a barrier lake approximately 5600 m long, 70 m high and 200 m wide. According to hydrological department calculations, the maximum flux was approximately 10000 m^3/s, posing a great threat to the lives and property of people in the downstream Jinsha River region.

(2) Case 2

On June 17th, 2020, a heavy rainstorm occurred in Danba County, Ganzi Prefecture, Sichuan Province, and a landslide occurred in Anangzhai village, which blocked the Xiaojinchuan River and caused the formation of a barrier lake. The barrier lake threatened more than 6000 people in 6 townships, 17 villages, 4 schools, 2 temples and 3 health centers downstream of the river.

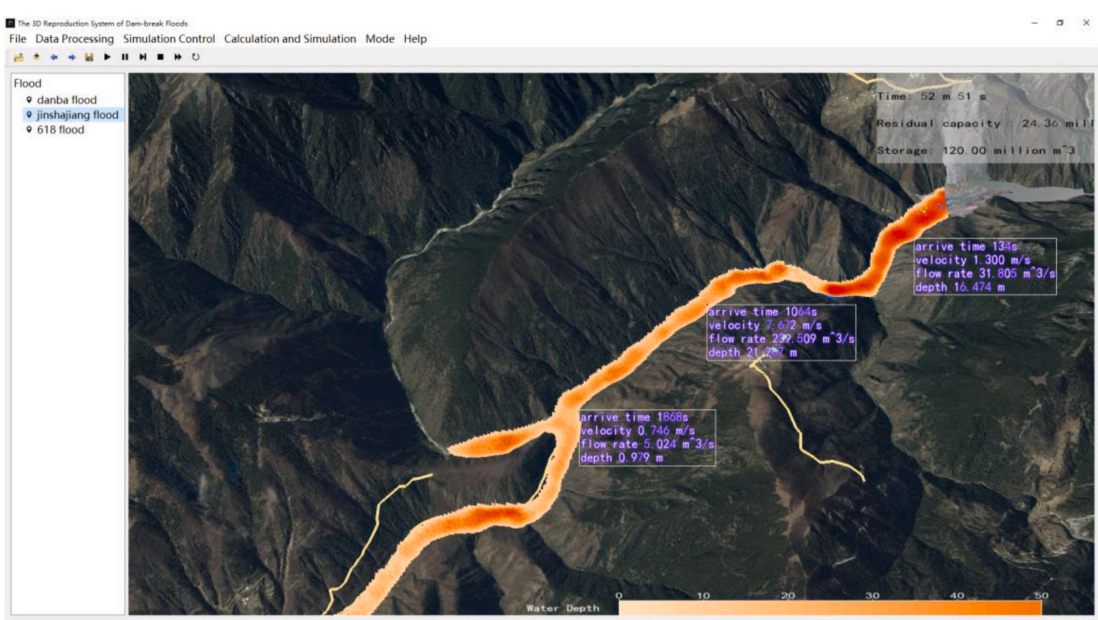

Fig. 7. The interface of the reproduction system.

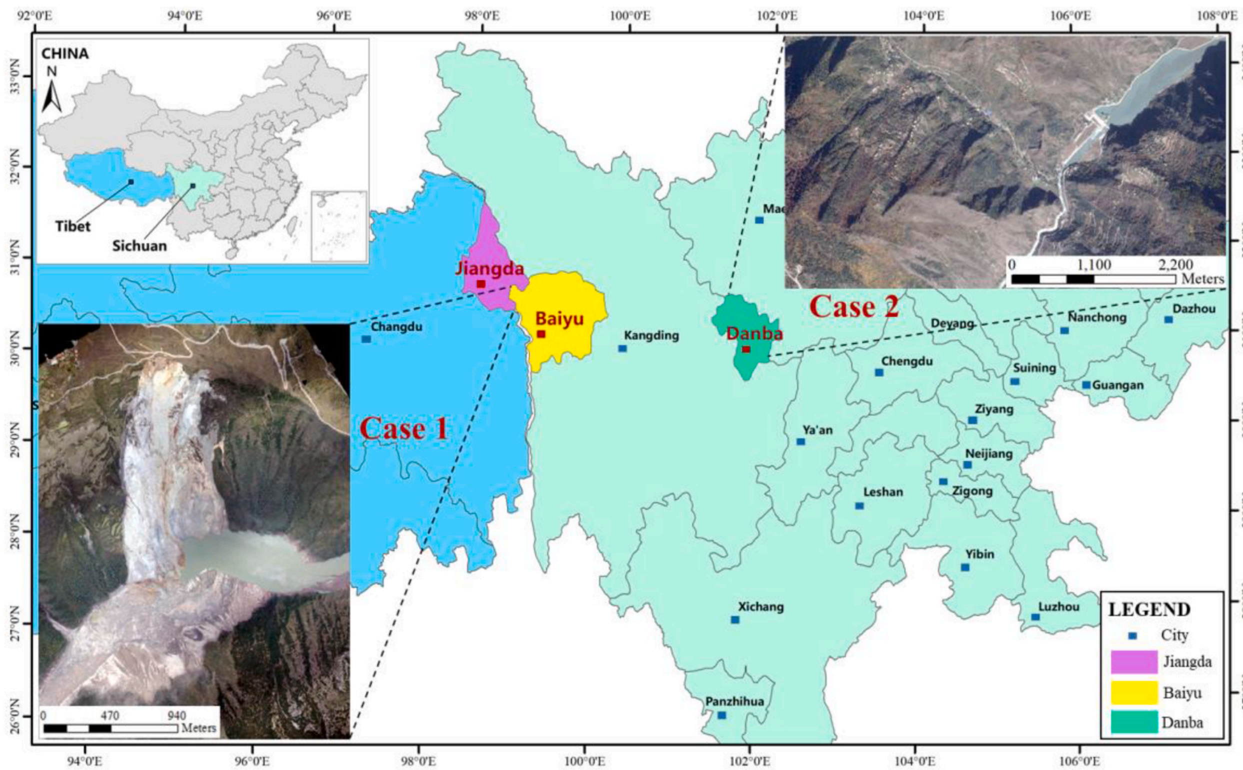

Fig. 8. Study area.

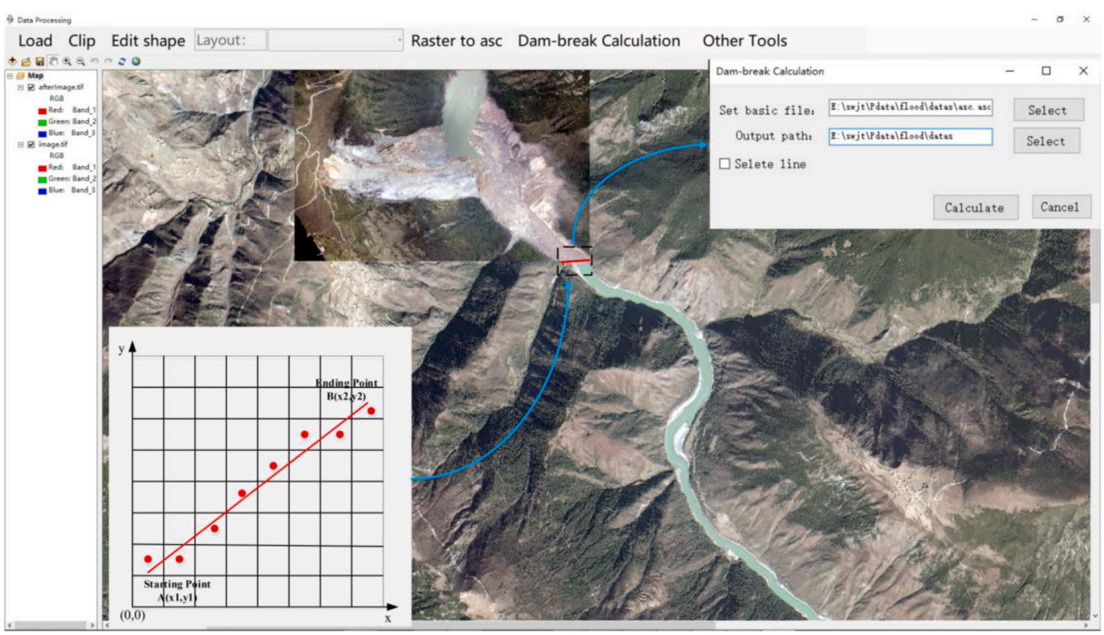

Fig. 9. Data processing tool.

4.3.2. Dam-break flood reproduction

(1) Data processing

The data processing tool was used to clip and project the geographical data and calculate the roughness value according to different types of features. Areas of road, river, farmland, grassland and residential land were assigned values of 0.016, 0.040, 0.035, and 0.070, respectively, by referring to Hossain et al. (2013) and Yin et al. (2017). Then, raster calculations were performed to merge these values into a roughness file and convert them to ASCII file format to save.

(2) The cell indexes of dam-break breach

The data preprocessing tool includes an acquisition module of cell indexes of dam-break breach, as shown in Fig. 9. We obtained the location and length of the dam break based on post-disaster images and DEM data, and formula (7) and formula (8) were used to calculate the

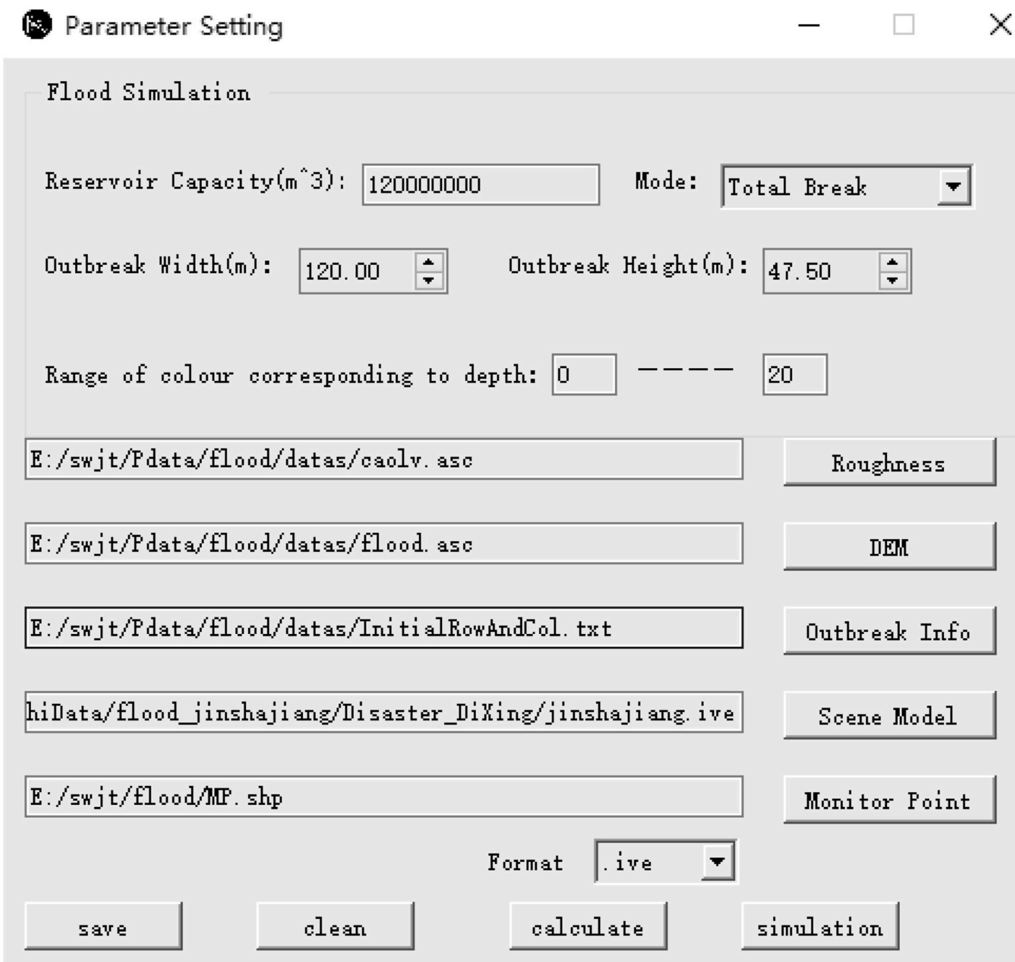

Fig. 10. Simulation parameter settings of dam-break floods.

direction and the number of grids, rows and columns. This information was used as input parameters for the dynamic reproduction of the dam-break flood.

$$\begin{cases} y = (x - x_1)k + y_1 \\ k = {y_2 - y_1}/{x_2 - x_1} \end{cases} \tag{7}$$

In the formula, k is the slope value, and (x,y) is the coordinate of an uncertain point. Then, formula (8) is used to obtain the row and column numbers of all dam-break cells.

$$\begin{cases} c = (x - x^{'})/g_{size} \\ r = t - (y - y^{'})/g_{size} \end{cases} \tag{8}$$

In the formula, r is the row number of the dam-break cell, c is the column number, $(x^{'},y^{'})$ is the geographic coordinates of the lower left corner, t is the total number of rows, and g_{size} is the grid size.

(3) Simulation parameter setting

The system provides a user-friendly parameter configuration interface, as shown in Fig. 10. Basic parameters include the storage capacity, dam-break width and height, and break mode. Simulation parameters include the roughness, DEM, and break value. Monitoring points are used to calculate and display real-time information such as arrival time, arrival location and remaining storage capacity.

(4) Reproduction and augmented representation of the whole process

First, the shaking of the 3D scene is used to indicate that the geological structure is loosened due to the impact of the earthquake. Soon afterward, a landslide is caused by intense rainfall, and the landslide deposits are buried in the river, causing the formation of a barrier lake. The visualization and description of the causes of the dam-break flood enhance the user's understanding of this flood type. Next, the spatio-temporal process of the dam-break flood is represented, including the water depth value at each moment, with the continuous yellow ribbon exhibiting one-to-one mapping. A darker color corresponds to a deeper flood. Additional information, such as the flood arrival time, arrival location, remaining storage capacity and flow velocity, is dynamically displayed. Finally, thematic information, such as the affected buildings and roads, is emphasized and highlighted, as shown in Fig. 11.

Fig. 12 shows the spatiotemporal development and trend of the dam-break flood in a VGE. Users can query the water depth, flow velocity, and submerged range at different times in real time. Fig. 13 shows the dam-break flood visualization in another case. More detailed experimental results in animated form in a video are available online (please see https://www.bilibili.com/video/BV15p4y1k7sM/and https://www.youtube.com/watch?v = WhKLYysEjm8).

4.3.3. Comparison with other flood systems

To highlight the innovation and advantages of the reproduction system of dam-break floods proposed in this paper, we compared the system with other flood simulation systems, as shown in Table 1. The

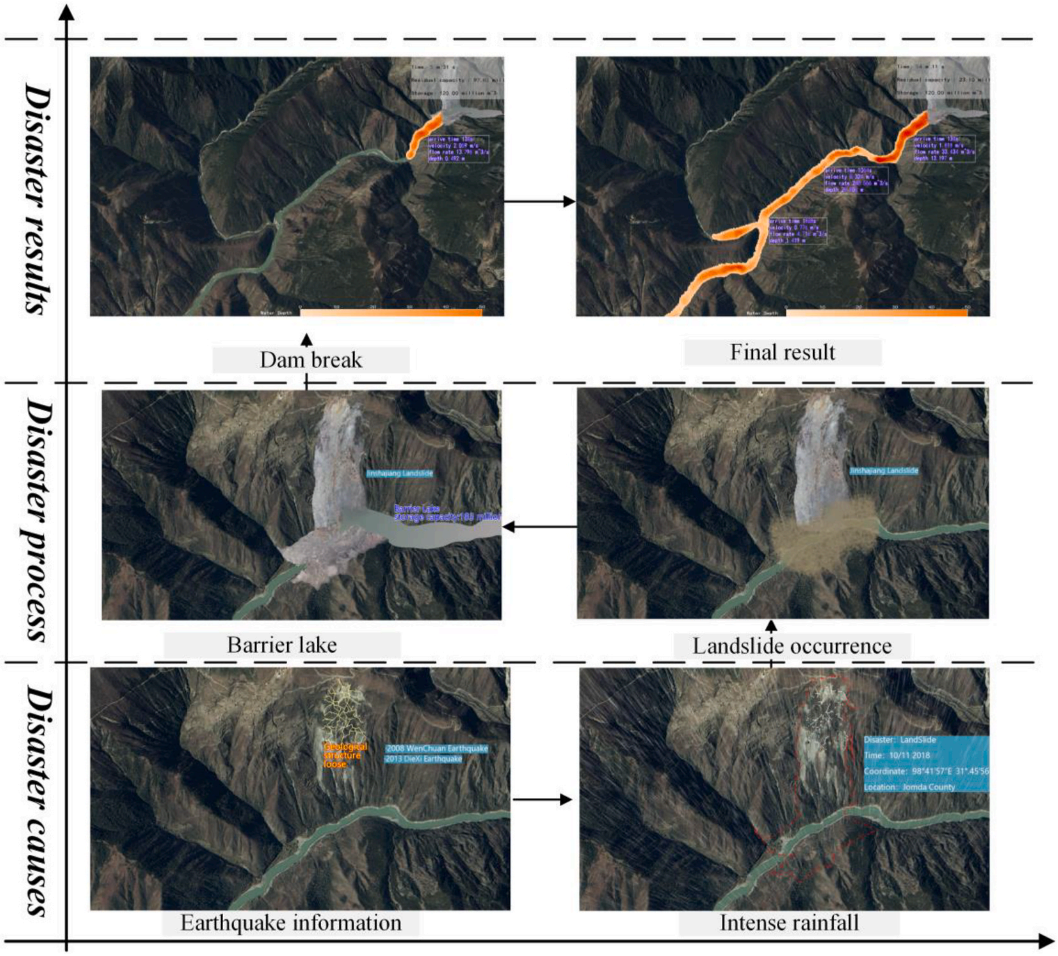

Fig. 11. Augmented representation of the whole process of a dam-break flood.

Fig. 12. The spatiotemporal process of a dam-break flood (case 1).

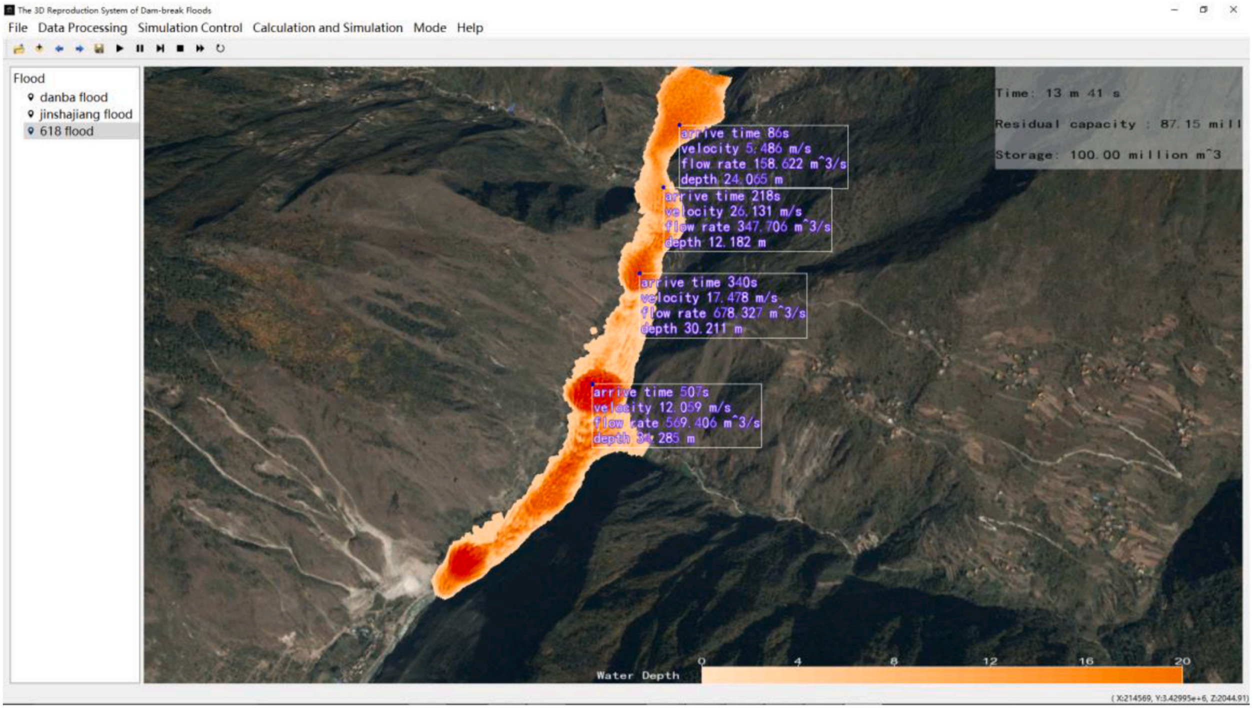

Fig. 13. The dam-break flood visualization in case 2.

Table 1
Advantages of the reproduction system of dam-break floods.

Analysis factor	The system in this article	MIKE	HEC-RAS	FlO-2D	Delft 3D
Number of input parameters	6	More than 10 professional parameters			
Reproduction time	Less than 1 h	3 h or longer			
Professional degree	Medium	High	High	High	High
Visual content	High	Medium	Medium	Low	High
3D dynamic visualization	Supported	Supported	Not supported	Not supported	Supported

results show that the reproduction system of dam-break floods proposed in this paper has the advantages of simple input parameters, a short reproduction time and a strong 3D visualization effect.

5. Discussion

In this paper, we aim to develop an efficient 3D reproduction and visualization system of dam-break floods. For additional inspiration and information to consider, the advantages and limitations of this system are discussed below.

First, the reproduction time of the flood process is reduced to less than 1 h by using our system. The simulation of the spatiotemporal process of a dam-break flood is a very complex process, and abundant input data and parameters are needed to achieve accurate simulation. The current flood system focuses on the mechanism and simulation accuracy and avoids a large time investment in data processing and simulation, which is inconsistent with the goal of rapid response to flood disasters. The rapid flood reproduction system simplifies the input parameters of the model and reduces the model calculation time. Furthermore, the system integrates input data processing, spatiotemporal simulation and augmented representation into a complete workflow, reducing the entire reproduction time of a dam-break flood process to one hour level and providing decision-making support for disaster response.

Second, this system supports rapid 3D reproduction of flood processes at different times and positions. A flexible parameter configuration is provided. The cross-section data, flow data, and dry and wet depth are required to set in the current flood simulation software, such as MIKE and the HEC series. The system proposed in this paper has a simplified parameter configuration, users only need to set several necessary parameters, such as the DEM, roughness and storage capacity. Furthermore, on this system, users can quickly visualize dam-break flood disasters at different times and locations. In addition, different from the current flood systems offered to professionals, the rapid dam-break flood system provides a user-friendly interface, hides potential technical details such as model calculations, and reduces user requirements with respect to professional background and experience. These advantages make the system applicable to the general public.

Third, augmented representation improves the transmission efficiency of flood disaster information. In the flood disaster management, users pay more attention to flood disaster information than to visual effects. Augmented representation allows visualization of the cause, process and result of dam-break floods through the combination of static representation and dynamic representation and a logical sequence, which can enhance the transmission of flood disaster information and the user's perception level.

Although we have invested much time and effort in system development, there is room for improvement. For example, the current computing framework of the dam-break reproduction uses mainly the CPU serial method, and each element is stored in an array. This framework will meet a challenge of low computational efficiency when processing large-scale and high-precision data, as described in the paper. Therefore, in upgrading the system, the computing framework could be extended to a parallel CPU and GPU framework. Moreover, the octree can be used to organize and manage the cell data to improve the computing efficiency of the dam-break model with high-precision DEM data. In addition, the current version of the system is a standalone system, we plan to modify the system architecture to a B/S structure and to provide flood disaster information service for more users.

6. Conclusions and future work

The rapid dam-break flood reproduction system is a platform developed to effectively represent disasters and disseminate information about disasters involving a dam-break flood. This system has the following characteristics. First, it supports the rapid processing of disaster information such as the disaster boundaries, dam-break location and roughness. Second, it integrates a numerical model of a dam-break flood based on CA to realize the spatiotemporal process simulation with the constraint of post-disaster information. Then, considering the whole process of a dam-break flood, it realizes augmented representation of the flood cause, the spatiotemporal process and the affected area based on the VGE, which improves the transmission efficiency of dam-break flood information. In addition, this system provides a flexible parameter configuration and a user-friendly interface to support typical users in simulating and displaying a dam-break flood process.

In future work, more disaster models, such as debris flows and landslides, will be integrated into this system. Furthermore, we plan to research ontology modeling of different disasters, clarify the complex semantic relationships between disaster objects, and reduce the difficulty of disaster 3D scene modeling and spatiotemporal process reproduction.

Software availability

The dam-break flood reproduction system was developed by Southwest Jiaotong University using C++ language on the Visual Studio 2010 platform. This system can be run on a standard PC. The software and part of the experimental data that support the findings of this study are available at figshare.com under the identifier https://figshare.com/s/a5026c73887472c3024f.

Declaration of competing interest

The authors declare that they have no known competing financial interests or personal relationships that could have appeared to influence the work reported in this paper.

Acknowledgements

This paper was supported by the National Natural Science Foundation of China (Grant Nos. U2034202, 41871289and 41941019) and Sichuan Science and Technology Program (Grant No. 2020JDTD0003).

Appendix A. Supplementary data

Supplementary data to this article can be found online at https://doi.org/10.1016/j.envsoft.2021.104994.

References

Achu, A.L., Aju, C.D., Reghunath, R., 2020. Spatial modelling of shallow landslide susceptibility: a study from the southern Western Ghats region of Kerala, India. Spatial Sci. 26 (2), 113–131. https://doi.org/10.1080/19475683.2020.1758207.
Bailey, J.E., Chen, A., 2011. The role of virtual globes in geoscience. Comput. Geosci. 37, 1–2.
Bainbridge, W.S., 2007. The scientific research potential of virtual worlds. Science 317 (5837), 472–476.
Bartholmes, J.C., Thielen, J., Ramos, M.H., Gentilini, S., 2009. The European flood alert system EFASePart 2: statistical skill assessment of probabilistic and deterministic operational forecasts. Hydrol. Earth Syst. Sci. 13, 141–153.
Carter, W.N., 2008. Disaster Management: A Disaster Manager's Handbook. 2008.
Chen, M., Lin, H., Wen, Y., Li, H., Hu, M.Y., 2013. Construction of a virtual lunar environment platform. Int. J. Digit. Earth 6 (5), 469–482.
Chen, M., Lin, H., Kolditz, O., Chen, C., 2015. Developing dynamic virtual geographic environments (VGEs) for geographic research. Environ. Earth Sci 74, 6975–6980.
Chen, M., Voinov, A., Ames, D.P., Kettner, A.J., Goodall, J.L., Jakeman, A.J., Barton, M. C., Harpham, Q., Cuddy, S.M., DeLuca, C., Yue, S., Wang, J., Zhang, F., Wen, Y., Lü, G., 2020. Position paper: open web-distributed integrated geographic modelling and simulation to enable broader participation and applications. Earth Sci. Rev. 207, 103–223.
Chen, M., Lin, H., 2018. Virtual geographic environments (VGEs): originating from or beyond virtual reality (VR)? Int. J. Digit. Earth 11 (4), 329–333. https://doi.org/10.1080/17538947.2017.1419452.
Cheng, R.Z., Chen, J., Cao, M., 2019. A virtual globe-based three-dimensional dynamic visualization method for gas diffusion. Environ. Model. Software 111, 13–23.
Ding, Y., Fan, Y., Du, Z., Zhu, Q., Wang, W., Liu, S., Lin, H., 2015. An integrated geospatial information service system for disaster management in China. Int. J. Digit. Earth 8, 918–945.
Domingo, N.D.S., Refsgaard, A., Mark, O., Paludan, B., 2010. Flood analysis in mixedurban areas reflecting interactions with the complete water cycle through coupled hydrological-hydraulic modelling. Water Sci. Technol. 62 (6), 1386–1392.
Ernst, J., Dewals, B.J., Detrembleur, S., Archambeau, P., Erpicum, S., Pirotton, M., 2010. Micro-scale flood risk analysis based on detailed 2D hydraulic modeling and high resolution geographic data. Nat. Hazards 55, 181–209.
Fan, Y.D., Wu, W., Wang, W., Liu, M., Wen, Q., 2016. Research progress of disaster remote sensing in China. J. Remote Sens. 20, 523–535.
FEMA, 2013. Geospatial Dam Break, Rapid EAP, Consequences and Hazards GIS Toolkit User Manual, Version 2.0.
Goodchild, M.F., 2004. GIScience, geography, form, and process. Ann. Assoc. Am. Geogr. 94, 709–714.
Granell, C., Díaz, L., Schade, S., Ostl€ ander, N., Huerta, J., 2013. Enhancing integrated environmental modelling by designing resource-oriented interfaces. Environ. Model. Software 39, 229–246.
Havenith, H., Cerfontaine, P., Mreyen, A., 2019. How virtual reality can help visualise and assess geohazards. Int. J. Digit. Earth 12 (2), 173–189.
Huang, J., Huang, R., Ju, N., Xu, Q., He, C., 2015. 3D WebGIS-based platform for debris flow early warning: a case study. Eng. Geol. 197, 57–66.
Kauffeldt, A., Wetterhall, F., Pappenberger, F., Salamon, P., Thielen, J., 2016. Technical review of large-scale hydrological models for implementation in operational flood forecasting schemes on continental level. Environ. Model. Software 75, 68–76.
Kaur, H., Gupta, S., Parkash, S., Thapa, R., Khanal, G.C., 2019. Evaluation of landslide susceptibility in a hill city of Sikkim Himalaya with the perspective of hybrid modelling techniques. Spatial Sci. 25 (2), 1113–1132.
Li, D.R., 2012. On space-air-ground integrated earth observation network. J. Geo-Inf. Sci. 14, 419–425.
Li, X., Liu, X.P., He, J.Q., et al., 2009. A geographical simulation and optimization system based on coupling strategies. Acta Geograph. Sin. 64 (8), 1009–1018.
Li, Y., Gong, J.H., Zhu, J., Ye, L., Song, Y.Q., Yue, Y.J., 2012. Efficient dam break flood simulation methods for developing a preliminary evacuation plan after the Wenchuan Earthquake[J]. Nat. Hazards Earth Syst. Sci. 12 (1), 97–106.
Li, Y., Gong, J.H., Liu, H., Zhu, J., Song, Y.Q., Liang, J.M., 2015. Real-time flood simulations using CA model driven by dynamic observation data. Int. J. Geogr. Inf. Sci. 29, 523–535.
Li, Y., Gong, J.H., Zhu, J., Song, Y.Q., Hu, Y., Ye, L., 2013. Spatiotemporal simulation and risk analysis of dam-break flooding based on cellular automata. Int. J. Geogr. Inf. Sci. 27, 2043–2059.
Li, Y., Zhu, Q., Fu, X., Feng, B., Liu, M.W., Zhang, J.X., Zhu, J., He, H.G., Yang, W.J., 2019a. Semantic visual variables for augmented geovisualization. Cartogr. J. 57 (1), 43–56.
Li, W.L., Zhu, J., Zhang, Y.H., Cao, Y.G., Hu, Y., Fu, L., Huang, P.C., Xie, Y.K., Yin, L.Z., Xu, B.L., 2019b. A fusion visualization method for disaster information based on self-explanatory symbols and photorealistic scene cooperation. ISPRS Int. J. Geo-Inf. 8, 104.
Li, W.L., Zhu, J., Fu, L., Zhu, Q., Xie, Y.K., Hu, Y., 2020. An augmented representation method of debris flow scenes to improve public perception. Int. J. Geogr. Inf. Sci. 1–24. https://doi.org/10.1080/13658816.2020.1833016。.
Lin, H., Chen, M., Lu, G., 2013a. Virtual geographic environment: a workspace for computer-aided geographic experiments. Ann. Assoc. Am. Geogr. 103 (3), 465–482.
Lin, H., Chen, M., Lu, G., Zhu, Q., Gong, J., You, X., Wen, Y., Xu, B., Hu, M., 2013b. Virtual geographic environments (VGEs): a new generation of geographic analysis tool. Earth Sci. Rev. 126, 74–84.
Lin, H., Chen, M., 2015. Managing and sharing geographic knowledge in virtual geographic environments (VGEs). Spatial Sci. 21 (4), 261–263.
Lu, G.N., Batty, M., Strobl, J., Lin, H., Zhu, A.X., Chen, M., 2019. Reflections and speculations on the progress in Geographic Information Systems (GIS): a geographic perspective. Int. J. Geogr. Inf. Sci. 33 (2), 346–367.
Pasquier, U., He, Y., Hooton, S., Goulden, M., Hiscock, K.M., 2018. An integrated 1D–2D hydraulic modeling approach to assess the sensitivity of a coastal region to compound flooding hazard under climate change. Nat. Hazards 94, 1–23.
Patel, D.P., Srivastava, P.K., 2013. A flood hazards mitigation analysis using remote sensing and GIS: correspondence with town planning scheme. Water Resour. Manag. 27, 2353–2368.
Pearce, L., 2003. Disaster management and community planning, and public participation: how to achieve sustainable hazard mitigation. Nat. Hazards 28, 211–228.

Price, D., Hudson, K., Boyce, G., Schellekens, J., Moore, R.J., Clark, P., Harrison, T., Connolly, E., Pilling, C., 2012. Operational use of a grid-based model for flood forecasting. P. I. Civ. Eng-Wat. M. 165, 65–77.
Qiu, L., Du, Z., Zhu, Q., Fan, Y., 2017. An integrated flood management system based on linking environmental models and disasters-related data. Environ. Model. Software 91, 111–126.
Sharma, P., Majumdar, S., 2016. Dam break analysis using HEC-RAS and HECGeoRAS- A case study of Ajwa reservoir. J. Water Resour. Ocean Sci. 5 (6), 108–133.
Shin, S., Her, Y., Song, J., Kang, M., 2019. Integrated sediment transport process modeling by coupling soil and water assessment tool and environmental fluid dynamics code. Environ. Model. Software 116, 26–39.
Symonds, A.M., Vijverberg, T., Post, S., van der Spek, B., Henrotte, J., Sokolewicz, M., 2016. Comparison between mike 21 FM, Delft3D and Delft3D FM flow models of western port bay, Australia. In: Proceedings of the 35th Conference on Coastal Engineering. Antalya, Turkey, 17–20 November.
Thakur, B., Parajuli, R., Kalra, A., Ahmad, S., Gupta, R., 2017. Coupling HEC-RAS and HEC-HMS in precipitation runoff modelling and evaluating flood plain inundation map. In: Proceedings of the World Environmental and Water Resources Congress 2017, pp. 240–251. Sacramento, CA, USA, 21–25 May 2017.
Waldman, S., Bastón, S., Nemalidinne, R., Chatzirodou, A., Venugopal, V., Side, J., 2017. Implementation of tidal turbines in MIKE 3 and Delft3D models of pentland firth & orkney waters. Ocean Coast Manag. 147, 21–36.
Wan, Z., Hong, Y., Khan, S., Gourley, J., Flamig, Z., Kirschbaum, D., Tang, G., 2014. A cloud-based global flood disaster community cyber-infrastructure: development and demonstration. Environ. Model. Software 58, 86e94.
Wang, Y., Chen, A.S., Fu, G., Djordjević, S., Zhang, C., Savić, D.A., 2018. An integrated framework for high-resolution urban flood modelling considering multiple information sources and urban features. Environ. Model. Software 5, 644–656.
Warren, I., Bach, H., 1992. MIKE 21: a modelling system for estuaries, coastal waters and seas. Environ. Software 7 (4), 229e40.
Wu, Y.H., Liu, K.F., Chen, Y.C., 2013. Comparison between FLO-2D and Debris-2D on the application of assessment of granular debris flow hazards with case study. J. Mt. Sci. 10, 293–304.
Yin, Z., Seo, D., 2016. Analysis of optimum grid determination of water quality model with 3-D hydrodynamic model using environmental fluid dynamics code (EFDC). Environ. Eng. Res. 21 (2), 171–179.
Zhu, J., Yin, L.Z., Wang, J.H., Zhang, H., Hu, Y., Liu, Z.J., 2015. Dam-break flood routing simulation and scale effect analysis based on virtual geographic environment. IEEE J. Sel. Top. Appl. Earth Obs. Remote Sens. 8, 105–113.